

- J. P. Wittke, Phys. Rev. Lett. **2**, 153 (1959).
- <sup>2</sup>H. J. Gerritsen, S. E. Harrison, and H. R. Lewis, J. Appl. Phys. **31**, 1566 (1960).
- <sup>3</sup>H. J. Gerritsen and H. R. Lewis, Phys. Rev. **119**, 1010 (1960).
- <sup>4</sup>H. J. Gerritsen and E. S. Sabisky, Phys. Rev. **125**, 1853 (1962).
- <sup>5</sup>H. J. Gerritsen and A. Starr, Arkiv Fysik **25**, 13 (1963).
- <sup>6</sup>E. Yamaka and R. G. Barnes, Phys. Rev. **135**, A144 (1964).
- <sup>7</sup>T. C. Ensign, Te-Tse Chang, and A. H. Kahn, Phys. Rev. **188**, 703 (1969).
- <sup>8</sup>E. Yamaka and R. G. Barnes, Phys. Rev. **125**, 1568 (1962).
- <sup>9</sup>H. G. Andresen, Phys. Rev. **120**, 1606 (1960).
- <sup>10</sup>D. L. Carter and A. Okaya, Phys. Rev. **118**, 1485 (1960).
- <sup>11</sup>Ru-Tao Kyi, Phys. Rev. **128**, 151 (1962).
- <sup>12</sup>Te-Tse Chang, Phys. Rev. **136**, A1413 (1964).
- <sup>13</sup>P. H. Kasai, Phys. Lett. **7**, 5 (1963).
- <sup>14</sup>C. Kikuchi, I. Chen, W. H. From, and P. B. Dorain, J. Chem. Phys. **42**, 181 (1965).
- <sup>15</sup>W. H. From, Phys. Rev. **131**, 961 (1963).
- <sup>16</sup>W. H. From, P. B. Dorain, and C. Kikuchi, Bull. Am. Phys. Soc. **9**, 244 (1964).
- <sup>17</sup>M. L. Harvill and R. Roy, *Crystal Growth*, edited by H. S. Peiser (Pergamon, Oxford, England, 1967), pp. 563-567.
- <sup>18</sup>M. L. Harvill, Ph. D. thesis (Pennsylvania State University, State College, Pa., 1966) (unpublished).
- <sup>19</sup>J. W. Goodrum, J. Cryst. Growth **7**, 254 (1970).
- <sup>20</sup>D. E. Swets, J. Cryst. Growth **8**, 311 (1971).
- <sup>21</sup>M. M. Faktor and J. I. Carrasso, J. Electrochem. Soc. **112**, 817 (1965).
- <sup>22</sup>D. P. Madacsi and O. R. Gilliam, Bull. Am. Phys. Soc. **17**, 572 (1972).
- <sup>23</sup>D. P. Madacsi and O. R. Gilliam, Phys. Lett. **41A**, 63 (1972).
- <sup>24</sup>T. Shimizu, J. Phys. Soc. Japan **23**, 848 (1967).
- <sup>25</sup>I. Siegel, Phys. Rev. **134**, A193 (1964).
- <sup>26</sup>T. Purcell and R. A. Weeks, Phys. Lett. **38A**, 473 (1972).
- <sup>27</sup>R. A. Breslow, Ph. D. thesis (University of Connecticut, Storrs, Conn., 1968) (unpublished).
- <sup>28</sup>M. Tinkham, Proc. Roy. Soc. (London) **A236**, 549 (1956).
- <sup>29</sup>F. Keffer, T. Oguchi, W. O'Sullivan, and J. Yamashita, Phys. Rev. **115**, 1553 (1959).
- <sup>30</sup>A. M. Clogston, J. P. Gordon, V. Jaccarino, M. Peter, and L. R. Walker, Phys. Rev. **117**, 1222 (1960).
- <sup>31</sup>R. E. Watson and A. J. Freeman, Phys. Rev. **134**, A1526 (1964).
- <sup>32</sup>I. Chen, C. Kikuchi, and H. Watanabe, J. Chem. Phys. **42**, 186 (1965).
- <sup>33</sup>F. Herman and S. Skillman, *Atomic Structure Calculations* (Prentice Hall, New York, 1963), Chap. 6. These tables list normalized radial wave functions  $P_n(r)$  obtained by the Hartree-Fock-Slater self-consistent atomic-field method.

## Electron-Spin-Resonance Spectra of Nearest-Neighbor $\text{Cr}^{3+}$ Pairs in the Spinel $\text{ZnGa}_2\text{O}_4$

J. C. M. Henning, J. H. den Boef, and G. G. P. van Gorkom

*Philips Research Laboratories, Eindhoven, Netherlands*

(Received 5 October 1972)

ESR spectra of nearest-neighbor  $\text{Cr}^{3+}$  pairs in  $\text{ZnGa}_2\text{O}_4$  are studied in detail at two frequency bands: X band (9.9 GHz) and Q band (32.5 GHz). Transitions within each of the spin multiplets  $\Sigma=1, 2$ , and 3 are observed. From the angular dependence of the spectra it is found that local lattice distortions due to Cr  $\rightarrow$  Ga substitution are negligible. The Cr-Cr coupling is described by the spin Hamiltonian:  $\mathcal{H}_{\text{ex}} = -J\vec{S}_1 \cdot \vec{S}_2 + j(\vec{S}_1 \cdot \vec{S}_2)^2 + A[\vec{S}_1 \cdot \vec{S}_2 - 3(\vec{S}_1 \cdot \vec{r}_{12})(\vec{S}_2 \cdot \vec{r}_{12})/r_{12}^3]$ . The temperature dependence of the ESR intensities is used to determine the coefficients of the bilinear ( $J$ ) and biquadratic ( $j$ ) exchange as,  $J/k = -(32 \pm 2)^\circ\text{K}$  (antiferromagnetic coupling),  $j/k = -(2 \pm 1)^\circ\text{K}$ . The anisotropic part of the coupling can be fully accounted for by magnetic dipole-dipole interaction:  $A = A_{\text{dip}} = +0.0675 \pm 0.0005 \text{ cm}^{-1}$ . The value of  $j$  can be explained on the basis of an exchange-striction model.

### I. INTRODUCTION

Knowledge of the basic exchange interactions between magnetic ions at  $B$  sites in normal spinels is a prerequisite for the understanding of the complicated ordering patterns commonly observed in these systems. Direct and detailed information about these interactions can be obtained from ESR and optical spectra of moderately dilute single crystals.<sup>1</sup>

In an earlier paper<sup>2</sup> we reported preliminary ESR data for the Cr-doped cubic normal spinel  $\text{ZnGa}_2\text{O}_4$ . The ionic radii of  $\text{Cr}^{3+}$  and  $\text{Ga}^{3+}$  are almost the same (0.63 and 0.62 Å, respectively) and the lattice parameter  $a = 8.330$  Å of the diamagnetic host<sup>3</sup> is nearly identical with that of the concentrated crystal  $\text{ZnCr}_2\text{O}_4$ , which has  $a = 8.327$  Å. Hence, little distortion is expected to occur as a consequence of the  $\text{Cr}^{3+} \rightarrow \text{Ga}^{3+}$  substitution.

Unfortunately, in Ref. 1 the assignment of the

ESR transitions to the spin multiplets  $\Sigma = 2$  and 3 was incorrect. As a matter of fact, the narrow, weak lines at  $H = 3036$  Oe and  $H = 3120$  Oe ( $\nu = 9684$  MHz and  $\vec{H} \parallel [111]$ ), which we attributed to ( $\Sigma = 2$ ;  $M = -1 \rightarrow -2$ ) transitions, do not belong to the pair system. Since they are present in the most concentrated (5-at.% Cr) crystals only, they might be due to Cr triads or more complex clusters.

In the present paper the ESR spectrum of nearest-neighbor Cr pairs in  $\text{ZnGa}_2\text{O}_4$  is reinvestigated. Transitions within each of the multiplets  $\Sigma = 1, 2$ , and 3 are observed and their temperature and angular dependences studied in detail. As a result, it is found that the lines with maximum intensity at  $T = 63$  °K, which in Ref. 1 were attributed to the multiplet  $\Sigma = 3$ , are in fact transitions within  $\Sigma = 2$ . The angular dependence of these lines reveals that the anisotropic part of the spin-spin coupling can be completely accounted for by magnetic dipole-dipole interaction, based on undistorted lattice separations.

Furthermore, the value of the bilinear exchange ( $J/k = -32$  °K), as deduced from the improved interpretation is in much better agreement with the asymptotic Curie temperature  $\Theta = -330$  °K of  $\text{ZnCr}_2\text{O}_4$ .<sup>4</sup> The value of the biquadratic exchange term ( $j/k = -2$  °K) is unaltered, and the original explanation in terms of Kittel's exchange-striction mechanism<sup>2</sup> remains valid.

## II. THEORY

The ESR spectrum of single  $\text{Cr}^{3+}$  ions at  $B$  sites has been studied earlier.<sup>5,6</sup> It can be described by an axial spin Hamiltonian

$$\mathcal{H}_i = g_{\parallel} \mu_B H_{z_i} S_{z_i} + g_{\perp} \mu_B (H_{x_i} S_{x_i} + H_{y_i} S_{y_i}) + D [S_{z_i}^2 - \frac{1}{3} S_i(S_i + 1)], \quad (1)$$

with  $S_i = \frac{3}{2}$ ,  $g_{\parallel} = 1.9776 \pm 0.0003$ ,  $g_{\perp} = 1.9867 \pm 0.0007$ , and  $D = +0.523 \pm 0.002$   $\text{cm}^{-1}$ . The center axes  $z_i$  ( $i = 1, 2, 3, 4$ ) are along the four local trigonal  $\langle 111 \rangle$  axes.

The geometry of nearest-neighbor (nn)  $B$  sites in normal spinel is illustrated in Fig. 1. The local trigonal axes of Cr ions Nos. 1 and 2 are denoted by  $Z$  and  $\zeta$ , respectively. They are not parallel, but include an angle of  $\gamma = 70^\circ 32'$ , so the Owen-Judd formulas<sup>7</sup> are not applicable to this case. The spin Hamiltonian of a nn Cr pair may be written

$$\mathcal{H}_p = \mathcal{H}_1 + \mathcal{H}_2 + \mathcal{H}_{\text{ex}}, \quad (2)$$

where  $\mathcal{H}_1$  and  $\mathcal{H}_2$  are single-ion spin Hamiltonians and  $\mathcal{H}_{\text{ex}}$  is the coupling term

$$\mathcal{H}_{\text{ex}} = -J \vec{S}_1 \cdot \vec{S}_2 + j (\vec{S}_1 \cdot \vec{S}_2)^2 + A [\vec{S}_1 \cdot \vec{S}_2 - 3(\vec{S}_1 \cdot \vec{r}_{12})(\vec{S}_2 \cdot \vec{r}_{12})/r_{12}^2], \quad (3)$$

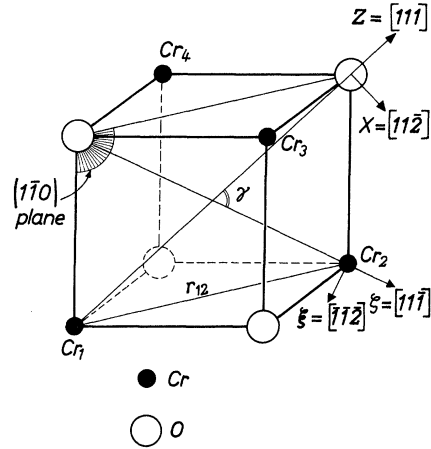


FIG. 1. Geometry of nn Cr pairs in spinel.  $Z$  and  $\zeta$  are the local trigonal axes of Cr ions Nos. 1 and 2, respectively.

which, in addition to the isotropic bilinear exchange also contains an isotropic biquadratic term and an anisotropic coupling of pseudodipolar form. Since the orbital singlet  ${}^4A_2$  ground state of octahedrally coordinated  $\text{Cr}^{3+}$  is far away from orbitally degenerate excited states, it may be expected that anisotropic exchange will be a relatively small effect. An estimate of the anisotropic exchange will be given in Sec. V A. Hence, the coefficient  $A$  will be mainly due to pure magnetic dipole-dipole interaction. For the same reason we omit anti-symmetric anisotropic exchange terms of the form  $\vec{D} \cdot (\vec{S}_1 \times \vec{S}_2)$ . In the undistorted lattice this term vanishes exactly since the point midway between the chromium ions is a center of symmetry.

The single-ion Hamiltonians  $\mathcal{H}_1$  and  $\mathcal{H}_2$  are not necessarily identical with Eq. (1) since the presence of a Cr ion instead of a Ga ion in the second-neighbor shell may give rise to an additional orthorhombic term  $E_p(S_x^2 - S_y^2)$  as well as to a modified coefficient  $D_p$  of the axial term. Formally we therefore write

$$\begin{aligned} \mathcal{H}_1 &= g \mu_B \vec{H} \cdot \vec{S}_1 + D_p [S_{z_1}^2 - \frac{1}{3} S_1(S_1 + 1)] \\ &\quad + E_p (S_{z_1}^2 - S_{y_1}^2), \\ \mathcal{H}_2 &= g \mu_B \vec{H} \cdot \vec{S}_2 + D_p [S_{z_2}^2 - \frac{1}{3} S_2(S_2 + 1)] \\ &\quad + E_p (S_{z_2}^2 - S_{y_2}^2). \end{aligned} \quad (4)$$

In Eqs. (4) and in what follows we disregard the small anisotropy in the  $g$  tensor, taking  $g = \frac{1}{3}(g_{\parallel} + 2g_{\perp})$ .

Since for nn pairs  $J \gg D_p, E_p, g \mu_B H$ , the total spin  $\vec{S} = \vec{S}_1 + \vec{S}_2$  is a good quantum number and it is convenient to rewrite both  $\mathcal{H}_{\text{ex}}$  and the Zeeman energy in terms of  $\Sigma$ . Furthermore, it is convenient to transform  $\mathcal{H}_2$  to the main axes of  $\mathcal{H}_1$  as follows:

$$\begin{aligned} S_{z2} &= S_{z2} \cos \gamma + S_{x2} \sin \gamma, \\ S_{x2} &= -S_{z2} \sin \gamma + S_{x2} \cos \gamma, \\ S_{y2} &= S_{y2}, \end{aligned} \quad (5)$$

where  $\gamma = 70^\circ 32'$  is the angle between  $z$  and  $\zeta$  and  $z$ ,  $\zeta$ ,  $x$ , and  $\xi$  are in the  $(1\bar{1}0)$  plane (see Fig. 1). We then find

$$\begin{aligned} \mathcal{H}_p &= -\frac{1}{2}J\Sigma(\Sigma+1) + \frac{1}{4}j\Sigma(\Sigma+1)[\Sigma(\Sigma+1) - 2S_1(S_1+1) - 2S_2(S_2+1)] \\ &+ g\mu_B\vec{H} \cdot \vec{\Sigma} + D_p[S_{z1}^2 + S_{z2}^2 \cos^2 \gamma + (S_{z2}S_{x2} + S_{x2}S_{z2}) \cos \gamma \sin \gamma + S_{x2}^2 \sin^2 \gamma] \\ &+ E_p[S_{x1}^2 - S_{y1}^2 + S_{z2}^2 \sin^2 \gamma + S_{x2}^2 \cos^2 \gamma - (S_{z2}S_{x2} + S_{x2}S_{z2}) \cos \gamma \sin \gamma - S_{y2}^2] \\ &+ \frac{1}{2}A[\frac{1}{4}(S_1^+S_2^- + S_1^-S_2^+) - S_{z1}S_{z2}](3 \cos \gamma + 1) \\ &- \frac{3}{4}A(S_{z1}S_{z2}^- + S_1^-S_{z2}^+) \sin \gamma - \frac{3}{4}A(S_{z1}S_2^+ + S_1^+S_{z2}^-) \sin \gamma \\ &- \frac{3}{8}A(S_1^-S_2^- + S_1^+S_2^+)(1 - \cos \gamma). \quad (6) \end{aligned}$$

We now proceed to calculate the eigenvalues and eigenvectors of  $\mathcal{H}_p$ . The first two terms in Eq. (6) give rise to four spin multiplets, characterized by  $\Sigma = 0, 1, 2$ , and  $3$  and with energies  $0, -J - \frac{1}{2}j$ ,  $-3J - \frac{27}{2}j$ , and  $-6J - 9j$ , respectively. The state vectors of the substates  $|\Sigma M\rangle$  can be expressed in terms of the single-ion states  $|m_1 m_2\rangle$  by using the Wigner coefficients:

$$|\Sigma M\rangle = \sum_{m_1} \sum_{m_2} (S_1 S_2 m_1 m_2 | \Sigma M) |m_1 m_2\rangle. \quad (7)$$

The results are given in Table I. Within this set of basis functions the matrix elements of  $\mathcal{H}_p$  are readily evaluated. They are presented in Table II.

It is to be noted that the matrix elements of the  $E_p$  and  $D_p$  terms in Eq. (6) are zero within the  $\Sigma = 2$  multiplet. (For the case of parallel center axes this property follows immediately from the Owen-Judd<sup>7</sup> formulas since  $\beta_2 = 0$ .) Hence, as long as multiplet mixing is unimportant, the transitions within  $\Sigma = 2$  are best suited to the study of any re-

maining anisotropic effects, as for instance the pseudodipolar  $A$  terms. If interaction between the multiplets is neglected the  $16 \times 16$  matrix factorizes into  $7 \times 7$ ,  $5 \times 5$ ,  $3 \times 3$ , and  $1 \times 1$  blocks. The blocks are readily diagonalized for various choices of  $D_p$ ,  $E_p$ , and  $A$  and for different orientations of  $\vec{H}$  by means of a computer program, based on the Housholder transformation.<sup>8</sup>

Finally, it can easily be seen that the principal axes of  $\mathcal{H}_p$  are along  $[110]$ ,  $[001]$ , and  $[\bar{1}10]$  for the pair  $\text{Cr}_1\text{-Cr}_2$  shown in Fig. 1, provided the following conditions are satisfied: (a) mixing between multiplets is negligible and (b)  $E_p \ll D_p$ .

### III. EXPERIMENTAL TECHNIQUES

The Cr-doped  $\text{ZnGa}_2\text{O}_4$  single crystals used in this work were identical with those used in earlier investigations.<sup>2,5</sup> They were grown from a  $\text{PbO-PbF}_2$  flux. The Cr concentration ranges from  $0.5 \times 10^{-2}$  to  $5 \times 10^{-2}$  g at./g mole  $\text{ZnGa}_2\text{O}_4$ . ESR spectra were recorded at two frequencies:  $\nu_1 = 9.900$  GHz ( $X$  band) and  $\nu_2 = 32.46$  GHz ( $Q$  band).

Since for the nearest-neighbor exchange interaction  $J$  will be much larger than  $g\mu_B H$ , mixing between the spin multiplets will be negligible. This implies that the values of  $J$  and  $j$  have to be determined from the temperature dependence of the ESR intensities, since the positions of the transitions within multiplets are independent of  $J$  and  $j$  to a high degree of accuracy.

In order to measure absorption intensities as a function of temperature one needs an ESR spectrometer with a constant sensitivity over a large temperature range ( $1-100^\circ\text{K}$ ). Both our  $X$ -band and  $Q$ -band spectrometers are of the homodyne mixer type.<sup>9</sup> If the sample volume is not too large, the cavity essentially remains matched to the waveguide even when the temperature is allowed to vary. Any slight deviation from the matched condition gives rise to a variation in the bias current of the detection crystal, and hence in the over-all spectrometer sensitivity. This may be compen-

TABLE I. State vectors of substates  $|\Sigma M\rangle$  for  $S_1 = S_2 = \frac{3}{2}$ , according to Eq. (7).

$\Sigma$	$\chi^a$	$ \Sigma M\rangle = \sum_{m_1} \sum_{m_2} (S_1 S_2 m_1 m_2   \Sigma M)  m_1 m_2\rangle^b$
3	+	$ 33\rangle =   \frac{3}{2}, \frac{3}{2} \rangle$
	+	$ 32\rangle = (2)^{-1/2} [   \frac{3}{2}, \frac{1}{2} \rangle +   \frac{1}{2}, \frac{3}{2} \rangle ]$
	+	$ 31\rangle = (6)^{-1/2} [   \frac{3}{2}, -\frac{1}{2} \rangle +   -\frac{1}{2}, \frac{3}{2} \rangle ] + (\frac{2}{3})^{1/2}   \frac{1}{2}, \frac{1}{2} \rangle$
	+	$ 30\rangle = (20)^{-1/2} [   \frac{3}{2}, -\frac{3}{2} \rangle +   -\frac{3}{2}, \frac{3}{2} \rangle ] + (\frac{6}{5})^{1/2} [   \frac{1}{2}, -\frac{1}{2} \rangle +   -\frac{1}{2}, \frac{1}{2} \rangle ]$
2	-	$ 22\rangle = (2)^{-1/2} [   \frac{3}{2}, \frac{1}{2} \rangle -   \frac{1}{2}, \frac{3}{2} \rangle ]$
	-	$ 21\rangle = (2)^{-1/2} [   \frac{3}{2}, -\frac{1}{2} \rangle -   -\frac{1}{2}, \frac{3}{2} \rangle ]$
	-	$ 20\rangle = (2)^{-1} [   \frac{3}{2}, -\frac{3}{2} \rangle +   \frac{1}{2}, -\frac{1}{2} \rangle -   -\frac{1}{2}, \frac{1}{2} \rangle -   -\frac{3}{2}, \frac{3}{2} \rangle ]$
1	+	$ 11\rangle = (\frac{3}{10})^{1/2} [   \frac{3}{2}, -\frac{1}{2} \rangle +   -\frac{1}{2}, \frac{3}{2} \rangle ] - (\frac{2}{5})^{1/2}   \frac{1}{2}, \frac{1}{2} \rangle$
	-	$ 10\rangle = (\frac{6}{5})^{1/2} [   \frac{3}{2}, -\frac{3}{2} \rangle +   -\frac{3}{2}, \frac{3}{2} \rangle ] - (20)^{-1/2} [   \frac{1}{2}, -\frac{1}{2} \rangle +   -\frac{1}{2}, \frac{1}{2} \rangle ]$
0	-	$ 00\rangle = (2)^{-1} [   \frac{3}{2}, -\frac{3}{2} \rangle -   \frac{1}{2}, -\frac{1}{2} \rangle +   -\frac{1}{2}, \frac{1}{2} \rangle -   -\frac{3}{2}, \frac{3}{2} \rangle ]$

<sup>a</sup> $\chi$  is the character under permutation of ions 1 and 2.

<sup>b</sup> $|\Sigma - M\rangle$  is obtained from  $|\Sigma M\rangle$  by sign reversal of all  $m_1$  and  $m_2$ ; an additional phase factor of  $-1$  has to be applied for  $\Sigma = 2$ , since  $(S_1 S_2 m_1 m_2 | \Sigma M) = (-1)^{\Sigma + S_1 + S_2} \times (S_1 S_2 - m_1 - m_2 | \Sigma - M)$ .

sated for by controlling the bias current through the detector crystal by means of an electronic device.<sup>10</sup> Another important point is the constancy

of the cavity  $Q$  factor. We obtained the best results with a quasirectangular  $TE_{102}$  cavity made of brass. The reason is that the temperature depen-

TABLE II. Matrix elements of  $\mathcal{H}_p$  within the basis  $|\Sigma M\rangle$ , defined in Table I. Off-diagonal elements between the spin multiplets are omitted. Definitions:  $u = \frac{1}{2}(3 \cos \gamma + 1)$ ,  $v = -\frac{3}{4} \sin \gamma$ ,  $w = -\frac{3}{8}(1 - \cos \gamma)$ . The coordinate axes,  $x$ ,  $y$ ,  $z$  are defined in Fig. 1.

$\Sigma$	$M$	$M'$	$\langle \Sigma M   \mathcal{H}_p   \Sigma M' \rangle$
1	1	1	$0.1 D_p(23 - 6 \cos^2 \gamma) - 0.6 E_p \sin^2 \gamma + 0.5250 uA + g\mu_B H_z$
	0	0	$0.1 D_p(29 + 12 \cos^2 \gamma) + 1.2 E_p \sin^2 \gamma + 3.0750 uA$
	-1	-1	$0.1 D_p(23 - 6 \cos^2 \gamma) - 0.6 E_p \sin^2 \gamma + 0.5250 uA - g\mu_B H_z$
	1	0	$-0.6(2)^{1/2}(D_p - E_p) \sin \gamma \cos \gamma + 2.4042 vA + g\mu_B(2)^{-1/2}(H_x - iH_y)$
	0	-1	$+0.6(2)^{1/2}(D_p - E_p) \sin \gamma \cos \gamma - 2.4042 vA + g\mu_B(2)^{-1/2}(H_x - iH_y)$
	-1	1	$-0.6 D_p \sin^2 \gamma - 0.6 E_p(\cos^2 \gamma + 3) + 0.2 wA$
	2	2	2
1		1	$+1.1250 uA + g\mu_B H_z$
0		0	$+1.8750 uA$
-1		-1	$+1.1250 uA - g\mu_B H_z$
-2		-2	$-1.1250 uA - 2g\mu_B H_z$
2		1	$+3vA + g\mu_B(H_x - iH_y)$
1		0	$+1.2247 vA + (\frac{3}{2})^{1/2} g\mu_B(H_x - iH_y)$
0		-1	$-1.2247 vA + (\frac{3}{2})^{1/2} g\mu_B(H_x - iH_y)$
-1		-2	$-3vA + g\mu_B(H_x - iH_y)$
2		0	$+2.4495 wA$
3	3	3	$1.5 D_p(2 + \cos^2 \gamma) + 1.5 E_p \sin^2 \gamma - 3.3750 uA + 3g\mu_B H_z$
	2	2	$2.5 D_p - 1.1250 uA + 2g\mu_B H_z$
	1	1	$0.1 D_p(22 - 9 \cos^2 \gamma) - 0.9 E_p \sin^2 \gamma + 0.2250 uA + g\mu_B H_z$
	0	0	$0.1 D_p(21 - 12 \cos^2 \gamma) - 1.2 E_p \sin^2 \gamma + 0.6750 uA$
	-1	-1	$0.1 D_p(22 - 9 \cos^2 \gamma) - 0.9 E_p \sin^2 \gamma + 0.2250 uA - g\mu_B H_z$
	-2	-2	$2.5 D_p - 1.1250 uA - 2g\mu_B H_z$
	-3	-3	$1.5 D_p(2 + \cos^2 \gamma) + 1.5 E_p \sin^2 \gamma - 3.3750 uA - 3g\mu_B H_z$
	3	2	$(\frac{3}{2})^{1/2} \sin \gamma \cos \gamma (D_p - E_p) + 3.6742 vA + 0.5(6)^{1/2} g\mu_B(H_x - iH_y)$
	2	1	$(\frac{3}{10})^{1/2} \sin \gamma \cos \gamma (D_p - E_p) + 2.8461 vA + 0.5(10)^{1/2} g\mu_B(H_x - iH_y)$
	1	0	$0.2(3)^{1/2} \sin \gamma \cos \gamma (D_p - E_p) + 1.0392 vA + 0.5(12)^{1/2} g\mu_B(H_x - iH_y)$
	0	-1	$-0.2(3)^{1/2} \sin \gamma \cos \gamma (D_p - E_p) - 1.0392 vA + 0.5(12)^{1/2} g\mu_B(H_x - iH_y)$
	-1	-2	$-(\frac{3}{10})^{1/2} \sin \gamma \cos \gamma (D_p - E_p) - 2.8461 vA + 0.5(10)^{1/2} g\mu_B(H_x - iH_y)$
	-2	-3	$-(\frac{3}{2})^{1/2} \sin \gamma \cos \gamma (D_p - E_p) - 3.6742 vA + 0.5(6)^{1/2} g\mu_B(H_x - iH_y)$
	1	3	$0.5(\frac{3}{5})^{1/2} D_p \sin^2 \gamma + 0.5(\frac{3}{5})^{1/2} E_p(3 + \cos^2 \gamma) + 2.3238 wA$
0	2	$(\frac{3}{10})^{1/2} D_p \sin^2 \gamma + (\frac{3}{10})^{1/2} E_p(3 + \cos^2 \gamma) + 3.2863 wA$	
-1	1	$0.6 D_p \sin^2 \gamma + 0.6 E_p(3 + \cos^2 \gamma) + 3.6000 wA$	
-2	0	$(\frac{3}{10})^{1/2} D_p \sin^2 \gamma + (\frac{3}{10})^{1/2} E_p(3 + \cos^2 \gamma) + 3.2863 wA$	
-3	-1	$0.5(\frac{3}{5})^{1/2} D_p \sin^2 \gamma + 0.5(\frac{3}{5})^{1/2} E_p(3 + \cos^2 \gamma) + 2.3238 wA$	

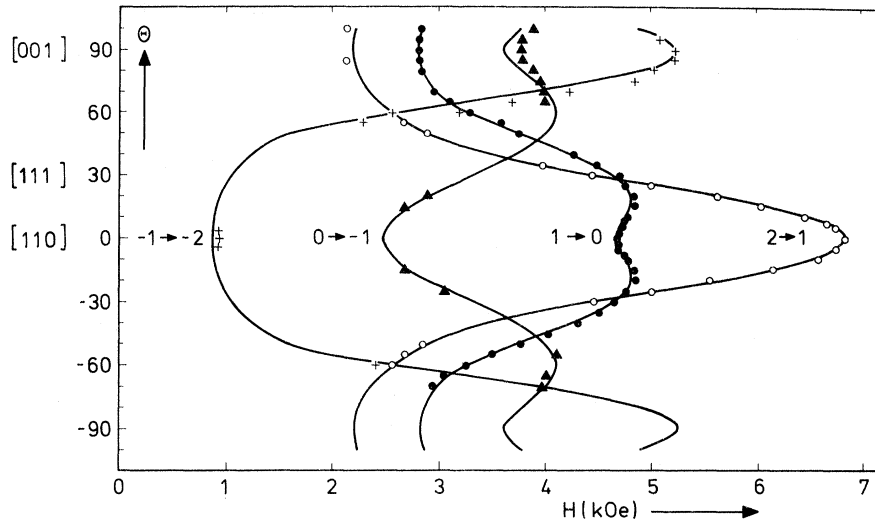


FIG. 2. Angular dependence of the four allowed transitions within  $\Sigma=2$  for  $\vec{H}$  rotating in a  $(1\bar{1}0)$  plane.  $T=77^\circ\text{K}$ ;  $\nu=9900\text{ MHz}$ . The theoretical curves (solid lines) are calculated with  $A=+0.0675\text{ cm}^{-1}$ .

dence of the Joule losses in the walls is much smaller for alloys than for pure metals. The overall spectrometer sensitivity was checked by simultaneously recording a  $-\frac{1}{2} \rightarrow +\frac{1}{2}$  transition of single  $\text{Cr}^{3+}$  ions, which is known<sup>5</sup> to obey a Curie  $1/T$  law. Deviations from a  $1/T$  behavior were always found to be within the experimental accuracy determined by random noise.

Temperature variation between 4.2 and about  $100^\circ\text{K}$  was achieved by allowing the cryostat to warm up after cooling with liquid helium. Typical warmup rates range from 0.2 to  $1.0^\circ\text{K}/\text{min}$ . The temperature was measured during each passage through a specific resonance line with a  $1000\text{-}\Omega$  Allen-Bradley carbon resistor mounted outside the cavity, as close as possible to the sample position. The temperature gradient  $\Delta T$  between the thermometer and the sample positions was measured in a dummy run, in which the sample was replaced by a second Allen-Bradley resistor. The maximum deviation was measured between  $T=4.2$  and  $6.0^\circ\text{K}$  and amounted to  $\Delta T=0.2^\circ\text{K}$ . Above  $T=6^\circ\text{K}$  the gradient was smaller than  $0.05^\circ\text{K}$ . The absolute accuracy of the temperature measurement is estimated as  $0.3^\circ\text{K}$ .

#### IV. RESULTS

##### A. Multiplet $\Sigma=2$

The most conspicuous pair lines, observed at  $T=77^\circ\text{K}$  are due to transitions within the  $\Sigma=2$  multiplet. Since the positions of these lines are independent of the parameters  $D_p$  and  $E_p$  (see Sec. II), they are well suited to determine the coefficient  $A$  of the pseudodipolar interaction. In addition, the angular dependence of the  $\Sigma=2$  spectrum gives information about the direction of the pair axis  $\vec{r}_{12}$ .

Figure 2 shows an angular diagram, taken with the X-band spectrometer ( $\nu=9900\text{ MHz}$ ), for  $\vec{H}$  rotating in the  $(1\bar{1}0)$  plane. In order to simplify the picture, only transitions of the specific pair  $\text{Cr}_1\text{-Cr}_2$  (see Fig. 1) are shown. As expected for nearest-neighbor pairs, the extrema are found to be along the  $[110]$  and  $[001]$  directions;  $[110]$  coincides with the pair axis  $\vec{r}_{12}$ .

The theoretical curves (solid lines) are calculated by diagonalizing the  $\Sigma=2$  block of the pair spin-Hamiltonian Eq. (6), using  $A=+0.0675\text{ cm}^{-1}$  and arbitrary values of  $D_p$  and  $E_p$ . The agreement between theory and experiment is good; especially the small dip predicted for the  $1 \rightarrow 0$  transition at  $\vec{H} \parallel [110]$  is reproduced very well by the experimental points. A more precise value of  $A$  was finally obtained by accurately measuring the line positions for  $\vec{H}$  along the pair axis  $[110]$ . We find

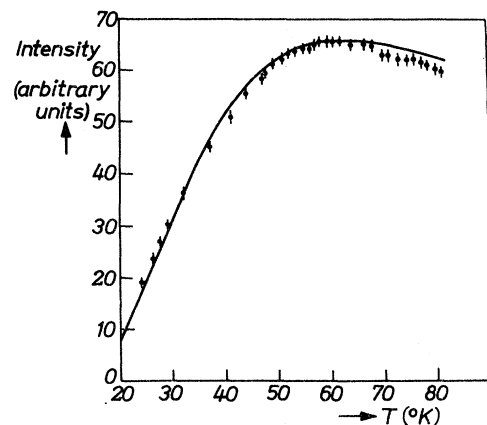


FIG. 3. Temperature dependence of the intensity of the  $(\Sigma=2; 1 \rightarrow 0)$  transition;  $\nu=9900\text{ MHz}$ . Solid line is the theoretical curve Eq. (8) with  $J/k=-32^\circ\text{K}$ ,  $j/k=-2^\circ\text{K}$ .

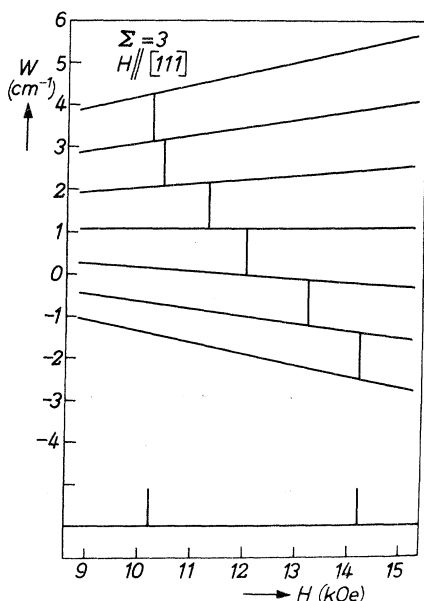


FIG. 4. Energy levels of the multiplet  $\Sigma=3$  as a function of  $H$  for  $\vec{H} \parallel [111]$  for the specific pair  $\text{Cr}_1 - \text{Cr}_2$ . Lower trace: observed transitions.

$$A = +0.0675 \pm 0.0005 \text{ cm}^{-1}.$$

The temperature dependence of the intensity of a ( $\Sigma=2$ ;  $1 \rightarrow 0$ ) transition is shown in Fig. 3. The experimental points are fitted to the expression

$$g_2 \propto (h\nu/kT) (Z)^{-1} e^{-W_2/kT}, \quad (8)$$

with

$$Z = 1 + 3e^{-W_1/kT} + 5e^{-W_2/kT} + 7e^{-W_3/kT} \quad (8a)$$

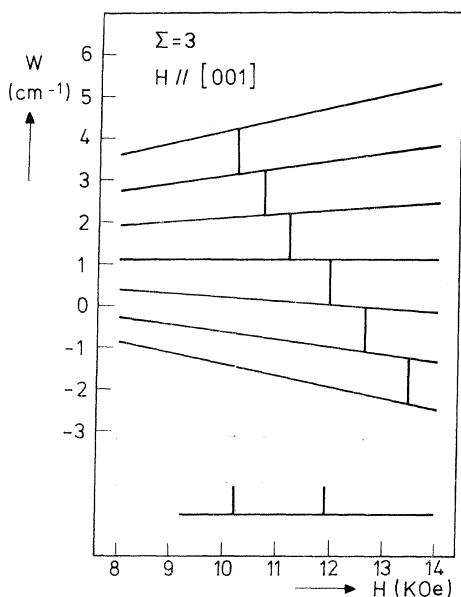


FIG. 5. Energy levels of the multiplet  $\Sigma=3$  as a function of  $H$  for  $\vec{H} \parallel [001]$  for the specific pair  $\text{Cr}_1 - \text{Cr}_2$ . Lower trace: observed transitions.

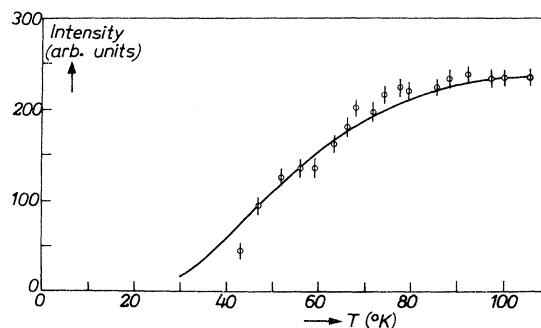


FIG. 6. Temperature dependence of the intensity of a transition within  $\Sigma=3$ ;  $\nu=32.46$  GHz. Solid line is the theoretical curve Eq. (9) with  $J/k=-32^\circ\text{K}$ ,  $j/k=-2^\circ\text{K}$ .

and

$$W_1 = -J - \frac{13}{2}j,$$

$$W_2 = -3J - \frac{27}{2}j,$$

$$W_3 = -6J - 9j.$$

The best fit is obtained for  $J/k = -(32 \pm 2)^\circ\text{K}$  and  $j/k = -(2 \pm 1)^\circ\text{K}$ . Introduction of  $j \neq 0$  improves the fit near the top of the curve, whereas the initial slope is determined by  $-J_{\text{eff}} = -J - \frac{9}{2}j$ .

The linewidth of the transitions within  $\Sigma=2$  is about 50 Oe and is independent of temperature for  $T < 300^\circ\text{K}$ . This means, that in the  $g-T$  plots the heights of the derivative lines could be used safely instead of intensities, thus avoiding double integration. The microwave power was always low enough to avoid saturation.

### B. Multiplet $\Sigma=3$

Transitions within  $\Sigma=3$  are an order less intense compared to those within the multiplet  $\Sigma=2$ . This is partly due to the Boltzmann factor and partly to a reduced transition probability. An additional complication arises from the fact that the zero-field splittings in the  $\Sigma=3$  multiplet are rather small (see Figs. 4 and 5), which implies that many of the  $\Sigma=3$  transitions will be in the neighborhood of the much stronger  $\Sigma=2$  lines.

Nevertheless, we have identified a couple of  $\Sigma=3$  lines at  $Q$ -band frequency when  $\vec{H}$  was along  $[111]$  and  $[001]$ , respectively. Figures 4 and 5 show that the positions of these lines are well described by the spin Hamiltonian Eq. (6) with  $D_p = D = +0.523 \text{ cm}^{-1}$  and  $E_p = 0$ .

The temperature dependence of the intensity of these lines is shown in Fig. 6. The theoretical curve given by Eq. (8a) and

$$g_3 \propto (h\nu/kT) (Z)^{-1} e^{-W_3/kT}, \quad (9)$$

with  $J/k = -32^\circ\text{K}$  and  $j/k = -2^\circ\text{K}$  gives good agreement with the experimental points.

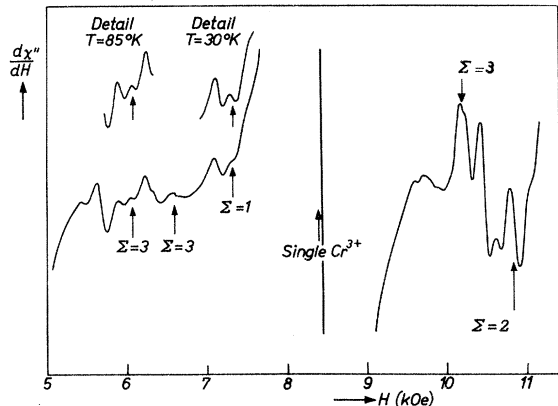


FIG. 7. Part of ESR spectrum at  $Q$  band ( $\nu=32.46$  GHz) for  $\vec{H} \parallel [001]$ ,  $T=77^\circ\text{K}$ , showing some of the pair transitions within  $\Sigma=1$ , 2, and 3.

The linewidth of the  $\Sigma=3$  lines is again 50 Oe, independent of temperature for  $T < 300^\circ\text{K}$ .

### C. Multiplet $\Sigma=1$

Transitions within the multiplet  $\Sigma=1$  are hard to find, in spite of the fact that the population of this multiplet is rather high. The reason is, that the transition probabilities are extremely small. As an example, for the ( $\Sigma=1$ ;  $-1 \rightarrow 0$ ) transition of the pair  $\text{Cr}_1\text{-Cr}_2$ , observed at  $\nu=32.46$  GHz, the

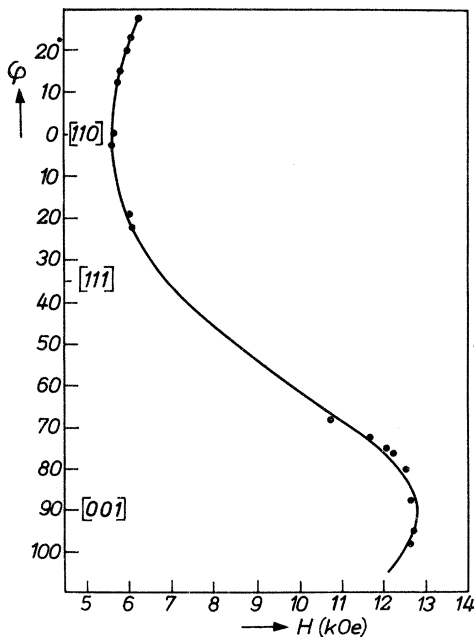


FIG. 8. Angular dependence of the ( $\Sigma=1$ ;  $-1 \rightarrow 0$ ) transition for  $\vec{H}$  rotating in the  $(1\bar{1}0)$  plane.  $T=77^\circ\text{K}$ ,  $\nu=32.464$  GHz. The theoretical curve (solid line) is calculated with  $A=+0.067$   $\text{cm}^{-1}$ ,  $D_p=D=+0.523$   $\text{cm}^{-1}$ , and  $E_p=0$ .

transition probability ranges from  $|\langle \varphi_{-1} | \Sigma_x | \varphi_0 \rangle|^2 = 0.05$  for  $\vec{H} \parallel [110]$  to 0.24 for  $\vec{H} \parallel [001]$ . The large zero-field splitting (over-all splitting 1  $\text{cm}^{-1}$ ) makes it necessary to study the transitions at  $Q$ -band frequencies. The relative strengths of some  $\Sigma=1$ , 2 and 3 lines are illustrated in Fig. 7.

Figure 8 gives the angular dependence of the ( $\Sigma=1$ ;  $-1 \rightarrow 0$ ) transition of the pair  $\text{Cr}_1\text{-Cr}_2$  for  $\vec{H}$  rotating in the  $(1\bar{1}0)$  plane. The theoretical curve (full line) was calculated by diagonalizing the  $\Sigma=1$  block of Eq. (6) with  $D_p=D=+0.523$   $\text{cm}^{-1}$  and  $E_p=0$ . Good agreement with the experimental line positions was obtained.

The experimental points plotted in Fig. 8 were selected on account of their temperature dependency. A typical result is presented in Fig. 9. The match to the theoretical curve, given by Eq. (8a) and

$$J_1 \propto (h\nu/kT) (Z)^{-1} e^{-W_1/kT} \quad (10)$$

with  $J/k = -32^\circ\text{K}$ ,  $j/k = -2^\circ\text{K}$ , is satisfactory, though not perfect. The discrepancies may be due to the fact that the  $\Sigma=1$  lines always appear as weak shoulders superimposed upon much stronger lines with a different (commonly  $1/T$ ) temperature dependence.

The linewidth of the  $\Sigma=1$  transitions is again of the order of 50 Oe. Apparently, the additional linebroadening mechanisms for the  $\Sigma=1$  and  $\Sigma=3$  transitions, presumed to be operative in the  $\text{KMgF}_3: \text{V}^{2+11}$  and  $\text{MgO}: \text{V}^{2+12}$  systems, are unimportant for  $\text{ZnGa}_2\text{O}_4: \text{Cr}^{3+}$ .

## V. DISCUSSION

### A. Lattice Distortion

Since the lattice parameters of  $\text{ZnGa}_2\text{O}_4$  and  $\text{ZnCr}_2\text{O}_4$  are almost identical, the relevance of the exchange parameters, as determined from measurements on dilute crystals, to the magnetic properties of the concentrated system mainly depends on the amount of local lattice distortion introduced

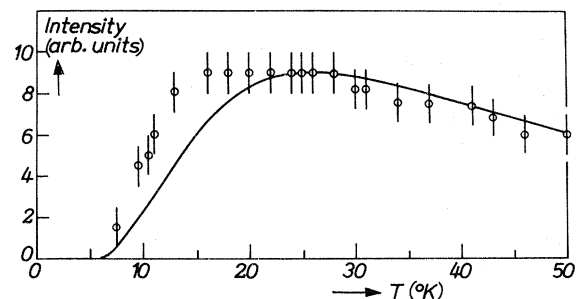


FIG. 9. Temperature dependence of the intensity of the ( $\Sigma=1$ ;  $-1 \rightarrow 0$ ) transition,  $\nu=32.46$  GHz. Solid line is the theoretical curve Eq. (10) with  $J/k = -32^\circ\text{K}$ ,  $j/k = -2^\circ\text{K}$ .

by the Cr-Ga substitution. There are two pieces of evidence that these distortions are very small indeed, in accordance with our initial expectation (see Sec. I).

First of all, the coefficient of the pseudodipolar coupling term  $A = +0.0675 \pm 0.0005 \text{ cm}^{-1}$  can be fairly well reproduced by a point-dipole calculation based on unmodified lattice separations ( $r_{12} = 2.94 \text{ \AA}$ ), which gives  $A_d \text{ (calc.)} = +0.0672 \text{ cm}^{-1}$ . [In fact, the value of  $A$  should be slightly different for different spin multiplets as a consequence of exchange striction (see Sec. VC). This effect has been recently observed by Harris<sup>13</sup> for  $\text{Mn}^{2+}$  pairs in  $\text{MgO}$  and  $\text{CaO}$ . In our case we were unable to detect it since a reliable  $A$  value could only be obtained from transitions in the  $\Sigma = 2$  multiplet.] Apart from dipole-dipole interaction, the empirical parameter  $A$  contains a small contribution  $A_{\text{an}}$  due to symmetric anisotropic exchange

$$A = A_d + A_{\text{an}} \quad (11)$$

An estimate of  $|A_{\text{an}}|$  is given by Moriya,<sup>14</sup>

$$|A_{\text{an}}| \approx (\Delta g/g)^2 |J| \approx 0.002 \text{ cm}^{-1} \quad (12)$$

Hence, it follows for the dipolar term:  $A_d = 0.067 \pm 0.002 \text{ cm}^{-1}$ , which means that the change in  $r_{12}$  due to Cr-Ga substitution is at most 1%.

The second argument in favor of the absence of distortions is the fact that the positions of the pair lines can be reproduced within the experimental accuracy by a spin Hamiltonian without orthorhombic terms:  $E_p = 0 \pm 0.006 \text{ cm}^{-1}$  and with  $D_p = D \pm 0.010 \text{ cm}^{-1}$ .

#### B. Bilinear Exchange

The values of the exchange constants, as determined in Sec. IV, are in excellent agreement with those obtained from optical spectra<sup>15</sup>  $J/k = -(31.9 \pm 0.7) \text{ }^\circ\text{K}$ ,  $j/k = -(2.4 \pm 0.5) \text{ }^\circ\text{K}$ . The accuracy of the optical method is slightly better since the exchange parameters are determined from the positions of the optical transitions rather than from the temperature dependence of their intensities. The  $J$  value ( $|J|/k = 4.28 \text{ }^\circ\text{K}$ ) determined by Begum and Murthy<sup>16</sup> from paramagnetic-neutron-scattering data on  $\text{ZnCr}_2\text{O}_4$  is in striking disagreement with our results.

It is interesting to see whether the asymptotic Curie temperature  $\Theta$  of  $\text{ZnCr}_2\text{O}_4$  can be explained on the basis of a nearest-neighbor interaction only. Values of  $\Theta$ , as determined from susceptibility measurements, have been reported by Baltzer *et al.*<sup>17</sup> ( $\Theta = -390 \text{ }^\circ\text{K}$ ), by Blasse and Fast<sup>18</sup> ( $\Theta = -350 \text{ }^\circ\text{K}$ ) and, more recently, by Kino and Lüthi<sup>4</sup> ( $\Theta = -330 \pm 10 \text{ }^\circ\text{K}$ ). With  $3k\Theta = 6S(S+1)J$  we find  $\Theta \text{ (calc.)} = -240 \text{ }^\circ\text{K}$ . So, 60–70% of the observed  $\Theta$  value can be accounted for by nearest-neighbor interaction. In order to explain the remaining 30–

40%, non-nearest-neighbor interactions have to be invoked.

#### C. Biquadratic Exchange

Biquadratic exchange terms in the coupling Hamiltonian may arise either from fourth-order transfer processes<sup>19,20</sup> or from exchange striction.<sup>21</sup>

The contributions due to transfer processes are in general very hard to calculate, but it has been pointed out by van Stapele<sup>22</sup> that for Cr-Cr pairs the leading term stems from fourth-order perturbation loops which involve low-spin states at an energy  $E_H$  (Hund energy,  $E_H \approx 1 \text{ eV}$ ) above the ground state. The resulting coefficient of the biquadratic exchange term  $j$  due to these transfer processes is of the order of<sup>22</sup>

$$j \approx +b^4/U^2 E_H \approx +J^2/E_H \quad (13)$$

where  $b$  is the appropriate transfer integral. From Eq. (13) it follows that transfer processes give rise to positive  $j$  values; the experimental value, however, is negative. Moreover, the value of  $j$  as calculated from Eq. (13) is an order too small:  $j/k \text{ [Eq. (13)]} = +0.10 \text{ }^\circ\text{K}$ . So, it is rather unlikely that transfer processes alone can account for the observed value of  $j$ .

An alternative mechanism leading to biquadratic

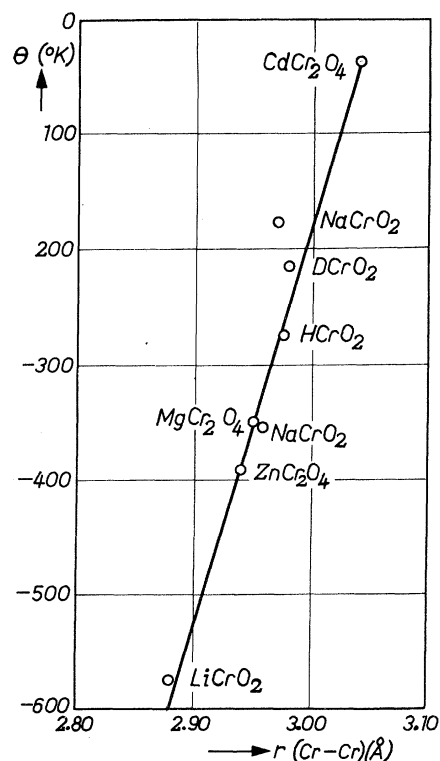


FIG. 10. Asymptotic Curie temperature  $\Theta$  vs interionic distance  $r(\text{Cr}-\text{Cr})$  according to Ref. 23.



terms has been proposed by Kittel.<sup>21</sup> Let us consider a pair of Cr ions embedded in a harmonic lattice. The free energy of the pair can be written as the sum of elastic and exchange terms

$$F = \frac{1}{2}cr_T(r - r_T)^2 - J\vec{S}_1 \cdot \vec{S}_2, \quad (14)$$

where  $c$  is the appropriate component of the elastic stiffness tensor. In the absence of exchange the equilibrium separation would be  $r_T$ . This separation is slightly modified by the exchange interaction. Putting  $\partial F/\partial r = 0$  we find

$$r = r_T + (J'/cr_T)(\vec{S}_1 \cdot \vec{S}_2), \quad (15)$$

where  $J' = dJ/dr$ . Substituting the new  $r$  value into Eq. (14) we finally find that the free energy contains a term proportional to  $(\vec{S}_1 \cdot \vec{S}_2)^2$  with a coefficient  $j$  given by

$$j = -\frac{1}{2}(J'^2/cr_T). \quad (16)$$

It should be noted that exchange striction gives rise to negative  $j$  values.

For 90° Cr-Cr interactions the striction effect

is of paramount importance because there is a subtle balance between positive superexchange (Cr-O-Cr) and negative direct exchange (Cr-Cr) interactions<sup>15</sup> resulting in a dramatically large value of  $J'$ . An estimate of  $J'$  can be obtained from the  $\Theta$  values of a number of chromites, as collected by Motida and Miyahara<sup>23</sup> (see Fig. 10). This plot of  $\Theta$  vs  $r$  leads to  $J' = 64 \times 10^{-7}$  erg/cm under the assumption that  $\Theta$  is mainly determined by nn interactions. With  $c = 20 \times 10^{11}$  dyn/cm<sup>2</sup> (mean value for spinel MgAl<sub>2</sub>O<sub>4</sub>) and  $r_T = 2.94 \times 10^{-8}$  cm, we arrive at the estimate  $j/k = -2.5$  °K, which is in excellent agreement with the experimental value.

#### ACKNOWLEDGMENTS

The authors are much indebted to R. P. van Stapele for stimulating discussions and to H. van den Boom for designing the microwave cavities and the temperature measuring setup and for calibrating the carbon-resistor thermometers by means of a computer program.

<sup>1</sup>J. C. M. Henning, in *Proceedings of the Ampère International Summer School II, Baško Polje, Yugoslavia*, 1971, edited by R. Blinc (Institute Jozef Stefan and University of Ljubljana, 1972), p. 179.

<sup>2</sup>J. C. M. Henning and J. P. M. Damen, *Phys. Rev. B* **3**, 3852 (1971).

<sup>3</sup>J. Hornstra and E. Keulen, *Philips Res. Repts.* **27**, 76 (1972).

<sup>4</sup>Y. Kino and B. Lüthi, *Solid State Commun.* **9**, 805 (1971).

<sup>5</sup>H. van den Boom, J. C. M. Henning, and J. P. M. Damen, *Solid State Commun.* **8**, 717 (1970).

<sup>6</sup>H. M. Kahan and R. M. Macfarlane, *J. Chem. Phys.* **54**, 5197 (1971).

<sup>7</sup>J. Owen, *J. Appl. Phys.* **32**, 213 (1961).

<sup>8</sup>R. S. Martin, C. Reinsch, and J. H. Wilkinson, *Num. Mathematik* **11**, 181 (1968); H. Bowdler, R. S. Martin, C. Reinsch, and J. H. Wilkinson, *Num. Mathematik* **11**, 293 (1968).

<sup>9</sup>T. H. Wilmshurst, *Electron Spin Resonance Spectrometers* (Hilger, London, 1967), p. 62.

<sup>10</sup>J. H. den Boef (unpublished).

<sup>11</sup>S. R. P. Smith and J. Owen, *J. Phys. C* **4**, 1399 (1971).

<sup>12</sup>A. J. B. Codling and B. Henderson, *J. Phys. C* **4**, 1409 (1971).

<sup>13</sup>E. A. Harris, *J. Phys. C* **5**, 338 (1972).

<sup>14</sup>T. Moriya, *Phys. Rev.* **120**, 91 (1960).

<sup>15</sup>G. G. P. van Gorkom, J. C. M. Henning, and R. P. van Stapele (unpublished).

<sup>16</sup>R. J. Begum and N. S. S. Murthy, *J. Phys. Chem. Solids* **33**, 759 (1972).

<sup>17</sup>P. K. Baltzer, P. J. Wojtowicz, M. Robbins, and E. Lopatin, *Phys. Rev.* **151**, 367 (1966).

<sup>18</sup>G. Blasse and J. F. Fast, *Philips Res. Repts.* **18**, 393 (1963).

<sup>19</sup>P. W. Anderson, in *Magnetism*, edited by G. T. Rado and H. Suhl (Academic, New York, 1963), Vol. I, p. 25.

<sup>20</sup>N. L. Huang and R. Orbach, *Phys. Rev. Letters* **12**, 275 (1964).

<sup>21</sup>C. Kittel, *Phys. Rev.* **120**, 35 (1960).

<sup>22</sup>R. P. van Stapele (private communication).

<sup>23</sup>K. Motida and S. Miyahara, *J. Phys. Soc. Japan* **28**, 1188 (1970).